Experimental Performance Limits on High Specific Impulse Ion Optics*

John D. Williams, D. Mark Laufer, and Paul J. Wilbur
Department of Mechanical Engineering
Colorado State University
Fort Collins, CO 80523
Phone: (970) 491-8564
FAX: (970) 491-8671
e-mail: johnw@engr.colostate.edu

ABSTRACT

Experiments are described that use sub-scale ion thruster optics (gridlets) that are comprised of 6 to 37 aperture pairs. Test results are used to determine limitations of several different ion optics systems that are operated at high net accelerating voltages of interest to high specific impulse ion thruster systems. Experimental results are compared to numerical and analytical electron backstreaming and perveance models. The importance of discharge chamber design to assure a flat ion beam current density profile is stressed in the context of maximizing thruster performance and avoiding the onset of destructive crossover and perveance limitations on beam current at beginning of life (BOL). Results will also be presented from related testing involving a neutralizer plasma probe to investigate electron backstreaming issues that develop at the end of life (EOL) in some mission scenarios. Judged from the ease of conducting the tests, we feel that gridlets can provide a quick and cost effective method for performing both (1) proof-of-design demonstration and (2) baseline evaluation of numerical models.

INTRODUCTION

The range of ion current that can be extracted through a single screen/accel grid hole pair with a given geometry and total accelerating voltage between the grids is limited. When this current is low, the sheath that separates the discharge chamber plasma from the ion acceleration region is dished upstream to the point where the ions are over-focused, their trajectories cross, and, at the limit, ions in the beamlet begin to impinge directly on the downstream edge of the accel grid barrel. When the beamlet current is high, on the other hand, the sheath is dished less, and the ions are sometimes under-focused to the point where they begin to impinge directly on the upstream edge of the accel grid barrel. These behaviors define the crossover and perveance limits on beamlets that are extracted over the full diameter of a given ion optics system.[1,2] Careful attention must be paid to these limits to prevent direct ion impingement and rapid accel grid erosion.[3,4]

A third and equally important operational limit for the grids is the voltage that must be applied to the accelerator grid to prevent electron backstreaming from the beam plasma. Ideally the accel grid voltage should be held negative of but as close to this limit as possible do damage due to the small current of charge exchange ions that sputter erode and limit the lifetime of this grid will be minimized. Unfortunately, the backstreaming limit can change as the accel grid wears over time, and compromises on selecting the magnitude of the accel voltage must be made. Many factors can affect the backstreaming voltage including beamlet current and aperture geometry. The flow field environment in the beam plasma is also an important factor in determining the backstreaming limit. It can be strongly affected by the operational conditions associated with the neutralizer and conductive plasma-bridge that forms between the neutralizer plasma and the beam plasma.

In this paper, we describe the experimental apparatus and procedures used to conduct tests on gridlets (typically 6- to 37-hole arrays). After the experimental setup and test procedures are described test results organized by gridlet type will be presented. Tests conducted on three widely different grid aperture styles are described that were conducted at specific impulse ranges of 2500 s to 4000 s, 3100 s to 6000 s, and 6000 s to 12,000 s. All of the gridlet results presented in this paper were obtained using xenon, and the main driver used to scale the low, medium, and high specific impulse grids was the inter-electrode electric field. The lower specific impulse gridlet set is based on a conventional SHAG (Small Hole Accel Grid) ion optics system that has been extensively utilized over the past 25 years. The medium specific impulse gridlet has been scaled up from the SHAG geometry and is referred to as the SUNSTAR geometry. Finally, those operated at the highest specific impulses, which have received some previous study by our group,[5] are designated the Interstellar Precursor (IP) gridlets.

* Presented as paper IEPC-03-128 at the 28th Int'l Electric Propulsion Conf., Toulouse, France, 17-21 March 2003.

APPARATUS AND PROCEDURES

A sketch of the gridlet test facility used during this study is shown in Fig. 1. Typical tests were conducted by mounting a two-grid, 6 to 37 aperture pair assembly to a ring-cusp discharge chamber. The grids were fabricated from graphite (Poco Graphite's high-purity, electronics grade AFX-5Q plate) using a computer controlled milling center. Depending upon size and voltage standoff requirements, the screen and accel gridlets were insulated from one another using either mica sheets or synthetic sapphire balls that were clamped between sputter-shielded brackets attached to the grids. The beam voltage applied to the screen grid and boosted bia the discharge chamber anode (not shown in Fig. 1) was measured relative to tank ground. It is noted that the inner diameter of the discharge chamber anode is 15 cm and this was quite a bit larger than the active diameter of the largest gridlet tested (4.7 cm). This was done to ensure that the discharge chamber plasma properties would be uniform over the entire gridlet area. And thereby impose common behavior in all beamlets and allow division of the measured beam current (J_B) by the number of apertures to obtain the beamlet current (J_b). A ground screen was placed between most of the inactive area of the accel grid and the beam plasma to limit the collection of beam plasma ions to this surface. The impingement current collected by the accel grid was measured using the ammeter shown in Fig. 1 (labeled J_A) and converted to a per beamlet value by dividing its reading by the number of accel grid apertures.

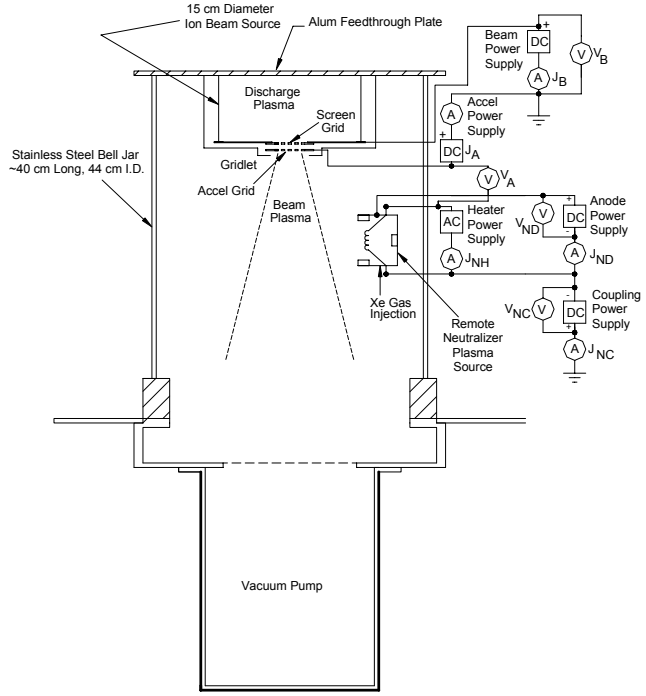

Fig. 1 Sketch of test apparatus showing gridlet ion source and neutralizer layout and wiring diagrams.

The ion beam was neutralized using a remotely located plasma source. It utilized a 6-cm diameter, ring-cusp-based ionization stage that was equipped with a hot filament cathode. This neutralizer plasma probe was operated over a very wide parameter space of flow rate, discharge power, and coupling bias to investigate the effects these parameters had on gridlet performance. The neutralizer discharge power could be controlled from 1 to 15 W at a discharge voltage of 30 V, the flow rate from 0.05 to 0.5 sccm, and the bias voltage from 0 to -40 V. Electron backstreaming can occur from the neutralizer directly through the ground screen to the gridlet ion source and care must be taken to avoid this. Tests conducted before and after a second ground screen was added to our test apparatus showed that a negatively biased surface placed between the perforated ground screen and the gridlet discharge chamber eliminated direct electron backstreaming through the ground screen from the neutralizer plasma flow field under normal operating conditions

The vacuum test facility was ~44 cm in diameter and was pumped by a diffusion pump equipped with a water-cooled baffle. No flow pressures were typically in the low 10^{-6} Torr range after baking the vacuum chamber for 1 to 2 hours. Xenon flow rates from ~30 to 150 mAeq induced pressures of $5x10^{-5}$ to $3x10^{-4}$ Torr. It is noted that larger vacuum facilities are available in our laboratory that would enable gridlet operation in the high 10^{-7} Torr pressure range. One such facility is also equipped with a diffusion pump, and its baffle is refrigeration-cooled to -70 °C.

The gridlets tests typically involved measurement of the beam current and accel current as the ion source discharge chamber power was varied. We fixed the discharge voltage to 30 V for all of the tests reported in this paper. We also fixed the flow rate at the start of a particular test to a value that was sufficiently larger than the rate required to operate at the perveance limit of the gridlet under test. Propellant utilization efficiencies at the perveance limit were typically between 50 and 75%. The gridlet tests were performed over wide ranges of both beam voltage and accel voltage to obtain throttling behavior and backstreaming data. In addition, studies of the neutralizer effect on the gridlet performance were conducted by varying the neutralizer plasma source operating and bias conditions.

RESULTS

Results obtained using SHAG, SUNSTAR, and IP gridlets are described in the subsections below. In general, the data are presented as functions of beamlet current, accel voltage, or in some cases as beamlet current density. Irregularly shaped apertures of gridlets in the SUNSTAR family are difficult to compare side by side or to the SHAG and IP results. In these instances, we have divided the beamlet current by the grid area (hole plus webbing) associated with an aperture (J_b/A_{tg}) and used this "beamlet current density" parameter to compare results. In the text, we also refer to normalized perveance per unit grid area and normalized perveance per hole, and these parameters are defined in Eqs. (1) and (2).

Normalized perveance ($\mathcal{P}_{tg}$) per unit grid area:

$$\mathcal{P}_{tg} = \frac{\left(\frac{J_b}{A_{tg}}\right)\frac{\ell_e^2}{V_T^{3/2}}}{\frac{4\varepsilon_o}{9}\sqrt{\frac{2e}{m}}} \qquad (1)$$

Normalized perveance per hole ($\mathcal{P}_h$):

$$\mathcal{P}_h = \frac{\left(\frac{4J_b}{\pi d_s^2}\right)\frac{\ell_e^2}{V_T^{3/2}}}{\frac{4\varepsilon_o}{9}\sqrt{\frac{2e}{m}}} \qquad (2)$$

The effective grid spacing (ℓ_e) and grid area per hole (A_{tg}) used in Eqs. (1) and (2) are defined as

$$\ell_e = \sqrt{(t_s + \ell_g)^2 + \frac{d_s^2}{4}} \quad \text{and} \quad A_{tg} = \frac{\ell_{cc}^2\sqrt{3}}{2}. \qquad (3)$$

The parameters in Eqs. (1), (2), and (3) are defined as follows: J_b represents the beamlet current, A_{tg} the grid area per hole, d_s the screen grid hole diameter, V_T the total voltage difference between the discharge plasma and the accel grid, ε_o the permittivity of free space, e the charge on an ion, m the mass of a xenon ion, t_s the thickness of the screen grid, l_g the spacing between the accel and screen grid, ℓ_{cc} the hole to hole spacing,, and d_s the screen hole diameter. It is noted that the beamlet current per unit grid area (J_b/A_{tg}) is equivalent to the total beam current per total grid area (J_B/A_{TG}) associated with the 6- to 37-hole gridlet under test.

SHAG Ion Optics- Low I_{sp}

Measurements were made on SHAG gridlets that demonstrated the importance of grid alignment on determination of the perveance limit, and these data are shown in Fig. 2a for a net accelerating voltage of 1.1 kV. Typical impingement data display a "U" shape when plotted as a ratio of impingement-to-beamlet current versus beamlet current as shown in Fig. 2a. Note that the beamlet current was varied in this experiment by varying the discharge current while holding the discharge, beam, and accel voltages constant. At low beamlet currents, the relative impingement current rises due to crossover ion impingement on the downstream edge of the accel hole barrels. At moderate beamlet currents, the relative impingement current is flat and at a value dependent upon the background neutral density and the propellant utilization efficiency of the ion source. In our small vacuum facility under low propellant utilization, the relative impingement current typically lies between 1 and 10% of the beam current. As the beamlet current is increased to higher values, the relative impingement current will again rise quickly indicating that direct ion interception is occurring on the upstream edge of the accel hole barrels due to perveance (or space-charge) limitations.

During the initial testing the SHAG gridlets were aligned visually with the aid of a microscope. The gridlet sets were disassembled and inspected after these preliminary tests and deposit patterns on the grids indicated that they were not aligned properly. In order to improve alignment quality, another SHAG gridlet set was machined out of graphite. This time alignment holes were added to ensure that the gridlets could be properly aligned, and Fig. 2a contains comparisons of crossover and perveance limit data sets for both the SHAG gridlet sets with and without alignment holes. Both gridlet sets were tested at the same operating conditions listed within the figure legend. It can be seen that the perveance limit was almost twice as high for the gridlet set equipped with alignment holes. The difference in the perveance limits was believed to be

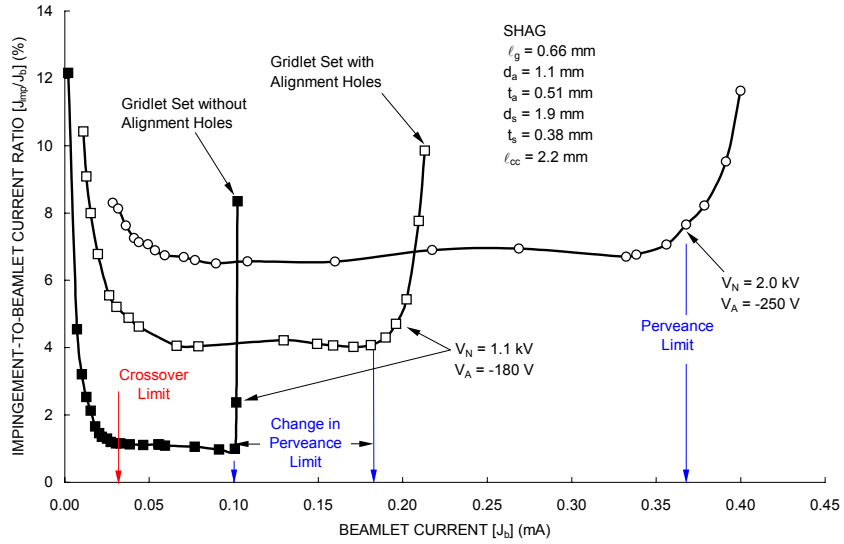

Fig. 2a Effects of alignment and applied voltage on perveance and crossover beamlet current limitations on SHAG optics.

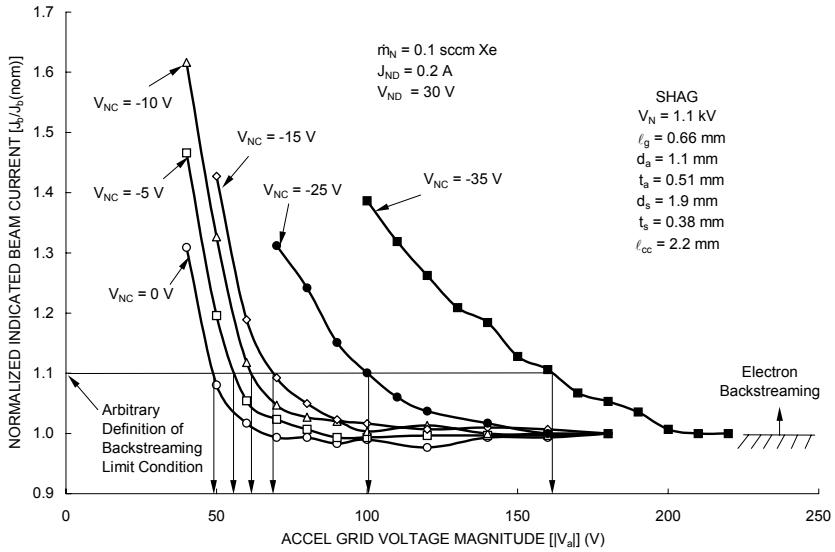

Fig. 2b Effects of neutralizer coupling bias on the onset of backstreaming for SHAG optics.

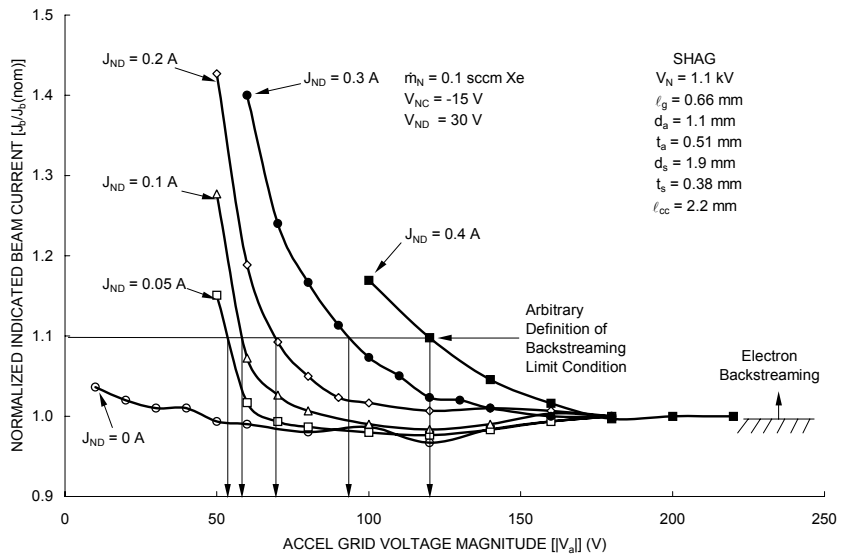

Fig. 2c Effects of neutralizer discharge power on the onset of backstreaming for SHAG optics.

due to what appeared to be modest misalignment between the holes during the original testing. Simulations performed with the ffx ion trajectory code[2] suggest that a hole-to-hole alignment offset of only 0.2 mm would be sufficient to cause the perveance limit differences shown in Fig. 2a. It is noted that the data in Fig. 2a for the gridlet set without alignment holes were collected at a flow rate of 0.1 sccm Xe. However, due to the increased perveance current limit, the gridlet set with alignment holes had to be tested at a much higher flow rate of 0.4 sccm Xe, in order to produce a high enough beam current to reach the higher perveance limit. This increased flow rate caused the level of impingement current to be higher throughout the range of beamlet currents investigated.

Another difference that was noted between the two 1.1 kV data sets shown in Fig. 2a was that the gridlet set with no alignment holes showed a much sharper transition between the safe zone and the perveance limit. This sharp increase in impingement current was also considered to be due to misalignment, because placement of the edges of accelerator holes closer to beamlet centerlines is believed to make them susceptible to more sudden interception of the tightly focused beamlet at the perveance condition corresponding to 0.1 mA per hole. Interestingly, the crossover limit measurement was found to be much less sensitive to grid alignment.

Figure 2a also contains a plot of impingement current data for the SHAG gridlet operated at a net voltage of 2 kV. The higher perveance current for this test was due to the much higher electric field operating condition. The normalized perveance per hole [P_h, Eq. (2)] at the perveance limit for the well-aligned gridlet at $V_N = 1.1$ kV was 0.57 and the value for $V_N = 2.0$ kV was 0.50.

The ability of an ion optics system to impart a negative potential throughout the beamlet volume near the axial location of the accel grid determines its capacity to stop beam plasma electrons from backstreaming into the discharge chamber. The geometry of a typical ion optics aperture set applies boundary conditions that result in an electrostatic potential saddlepoint being formed near the axial location of the accel grid on the beamlet centerline. This saddlepoint presents the least resistance path to electrons on trajectories that could carry them from the beam plasma toward the discharge plasma. Experiments were performed on the SHAG gridlet to determine the effect of the neutralizer plasma probe operating conditions on the beam plasma electrons and their ability to tunnel through the saddlepoint potential. In these tests the backstreaming limit was arbitrarily defined as the accel voltage at which apparent beam current (enhanced via electron backstreaming) had increased to a value that was 10% greater than the beam current measured at the nominal accel voltage condition. In one experiment, the effects of varying the neutralizer bias potential (coupling voltage) on the backstreaming limit were investigated for a beam current setting that was at the midpoint between the crossover and perveance limits. Figure 2b shows the results obtained during this experiment. (It is noted that the accel voltage and backstreaming limits discussed below and presented in Fig. 2 were measured relative to the vacuum facility ground to remove any confusion that might result during tests using different coupling voltages.) With no bias maintained on the neutralizer cathode, the backstreaming limit was found to be approximately -49 V. The magnitude of this measured backstreaming voltage (49 V) was significantly lower than that predicted from analytical models[6] (106 V) presumably because the 0 V bias condition does not produce electrons with sufficient energy to easily tunnel from the neutralizer location through the accel grid holes. We note that if a beam current criterion less than 10% was used, higher backstreaming magnitudes would result from our data.

As the neutralizer coupling voltage was varied from 0 to 10 V below ground, the magnitude of the backstreaming limit voltage increased linearly to approximately 61 V. However, as the neutralizer was biased more negative, the backstreaming limit started to increase rapidly (e.g. changing the neutralizer coupling voltage from -10 V to -35 V caused the backstreaming limit to change from 61 V to 160 V). The data in Fig. 2b suggest that electrons produced at voltage magnitudes ~25 V or more below ground can readily flow from the neutralizer plasma source and tunnel through the accel grid unless the accel grid is more negative than 100 V. It is noted that the strong sensitivity of backstreaming onset to the neutralizer operating condition shown in Fig. 2b may help explain BOL backstreaming limit differences that are observed on identical flight thrusters that exhibit slightly different neutralizer coupling voltages.

Similar experiments were performed in which the onset of backstreaming was investigated as a function of the neutralizer plasma production rate. Figure 2c shows the effect of neutralizer discharge current on the backstreaming limit for the case where the discharge voltage was held constant at 30 V. In these experiments, it was found that with no neutralizer plasma production ($J_{ND} = 0$ A), the onset of backstreaming could not be determined (presumably because the self-generated beam plasma was not capable of supplying sufficient electron current to the region near the gridlet). However, when the neutralizer discharge current was increased to just 0.05 A (a discharge power of only 1.5 W), the backstreaming limit was found to be well defined at 52 V. As the neutralizer discharge current, and, consequently, the neutralizer

plasma production rate, was increased, the backstreaming limit was observed to grow increasingly in magnitude. We judge that this behavior may have important design constraint implications in a centralized neutralizer system that is designed to neutralize an array of ion thrusters through the creation of relatively dense plasma. Here we are implying that a thruster located adjacent to the centralized neutralizer may experience backstreaming onset sooner than thrusters located further away due to locally higher beam plasma densities.

SUNSTAR Ion Optics- Medium I_{sp}

Four gridlet sets, designated SUNSTAR, were designed and fabricated to be operated over a specific impulse range from ~3000 s to 6000 s . Numerical simulations corresponding to the geometries of the SUNSTAR gridlets are presented in Ref. [2] along with specific design information. All four of the SUNSTAR grid designs have the same ion extraction area and web width, but different aperture configurations. Figure 3 shows photographs of the screen and accelerator gridlets for each of the different configurations. The screen grids of the two gridlet sets shown along the top row in Fig. 3, identified as the hex and square pattern gridlets, both have thirty-six 3.1-mm diameter holes corresponding to a screen open area (A_{so}) of 2.63 cm^2. Both gridlet sets also display the same web width (0.5 mm) between the screen holes. The only difference between the two, which is obvious from the photos, is the layout of the thirty-six holes. The hex pattern holes are staggered, resulting in a hexagonal arrangement of adjacent holes surrounding each hole except those on the periphery. The square pattern holes are all aligned, resulting in a square arrangement of adjacent holes surrounding each hole except those at the edge. The other two SUNSTAR gridlet sets, the long-slot and short-slot patterns, were designed to have the same ion extraction area as the hex and square patterns (2.63 cm^2). Each screen grid slot has the same width as the hole diameter in the aforementioned grids. The long-slot pattern has six slots, 12-mm long yielding 2.63 cm^2 of open area. The short-slot pattern has twelve slots, 4.8-mm long, again yielding 2.63 cm^2 of open area. The width of the webs between each slot is again 0.5 mm.

Experiments have been performed on each of the SUNSTAR gridlet sets to find the effect of throttling the net acceleration voltage. These tests were performed at 5 different operating conditions over a range of specific impulse from 3100 s to 6000 s. The following equation defines the relationship between specific impulse and net accelerating voltage.

$$I_{sp} = (2eV_N/m_+)^{1/2}(\eta_u/g_{eo}) \qquad (4)$$

In Eq. (4), I_{sp} represents to specific impulse in seconds, V_N the net accelerating voltage, η_u the utilization efficiency (assumed conservatively to be 75%), e the charge of an electron, m the mass of a xenon ion, and g_{eo} the gravitational acceleration constant. The following values of specific impulse correspond to the net accelerating voltages used during the SUNSTAR gridlet tests:

3,100 s Isp – 1.1 kV	3,600 s Isp – 1.5 kV	4,050 s Isp – 1.9 kV
5,000 s Isp – 2.9 kV	6,000 s Isp – 4.2 kV	

Measurements of the backstreaming limit were performed for each of the SUNSTAR gridlet sets and typical results are shown in Fig. 4. This was done by setting the beam current to an initial value that was a few milliamperes below the perveance limit when the accelerator grid voltage was at -250 V for the 4050 s specific impulse operating condition (Fig. 4a). The accelerator voltage magnitude was then decreased incrementally and the beam current was recorded at each voltage. The ratio of the beamlet current to the original beamlet current at -250 V (J_b/J_b[nom]) was then plotted against accel grid voltage magnitude ($|V_a|$) to obtain the plot shown in Fig. 4a. For these data the backstreaming limit was arbitrarily defined as the accelerator grid voltage at which the beam current increases five percent above of its initial value under the assumption that the current increased due to electrons backstreaming from the beam plasma region into the discharge plasma. The figure shows the square and hex pattern gridlets are very similar as they both begin to backstream at about the same voltage magnitude, (66 and 72 V). The short- and long-slot pattern grids require greater voltage magnitudes (172 and 177 V, respectively) to prevent electron backstreaming. It is postulated that the backstreaming limits differ because of the difference in the proximity of the accel grid surface to the region through which electrons backstream. For the test results presented in Fig. 4, the neutralizer discharge power, flow rate, and coupling voltage were set to 6 W (30 V at 0.2 A), 0.1 sccm (Xe), and -15 V, respectively. We note that the accel voltage presented in Fig. 4 and discussed above was measured relative to the neutralizer cathode for this test, which is the commonly accepted method of reporting this parameter. A backstreaming measurement of 66 V in Fig. 4 corresponds to an accel voltage of -66 V relative to the neutralizer cathode and -81 V [V_A+V_{NC}= (-66 + -15) V] relative to tank ground. It is noted that both of the backstreaming limit measurements shown in Fig. 4a for the hex and square layout

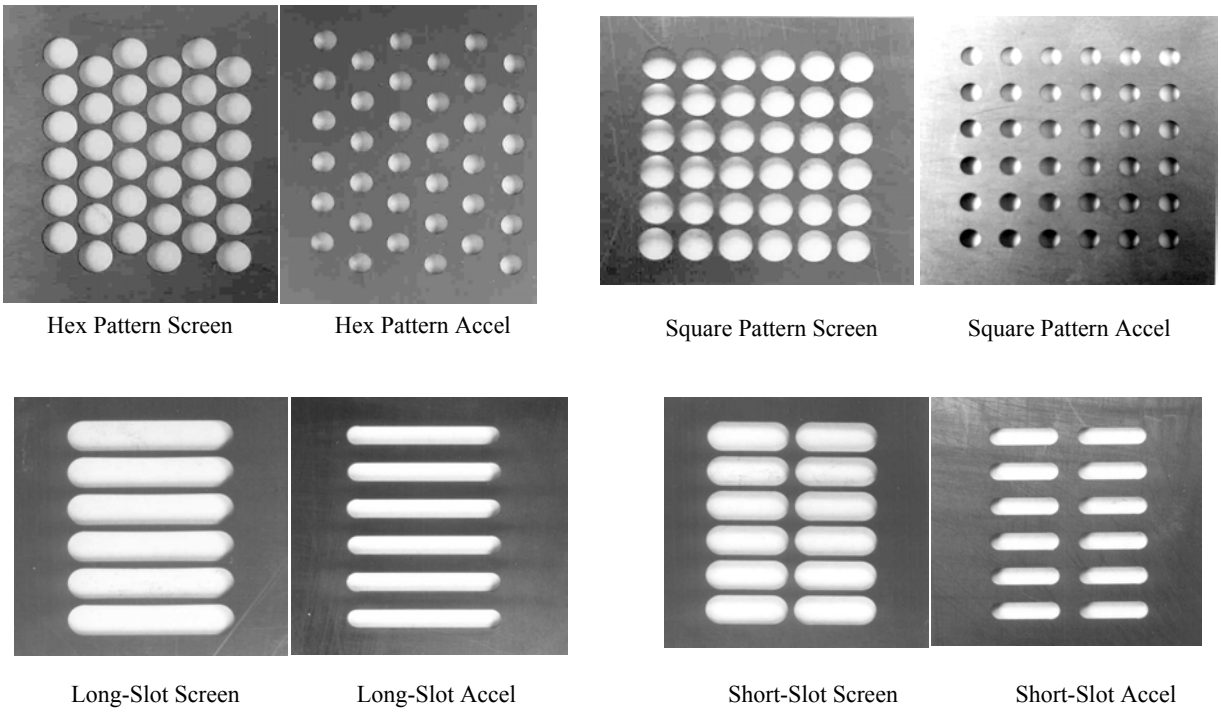

Fig. 3 Photographs of SUNSTAR gridlet pairs fabricated from Poco graphite using computer controlled milling center.

Fig. 4a Typical backstreaming limit data for the SUNSTAR gridlets operated at 4050 s.

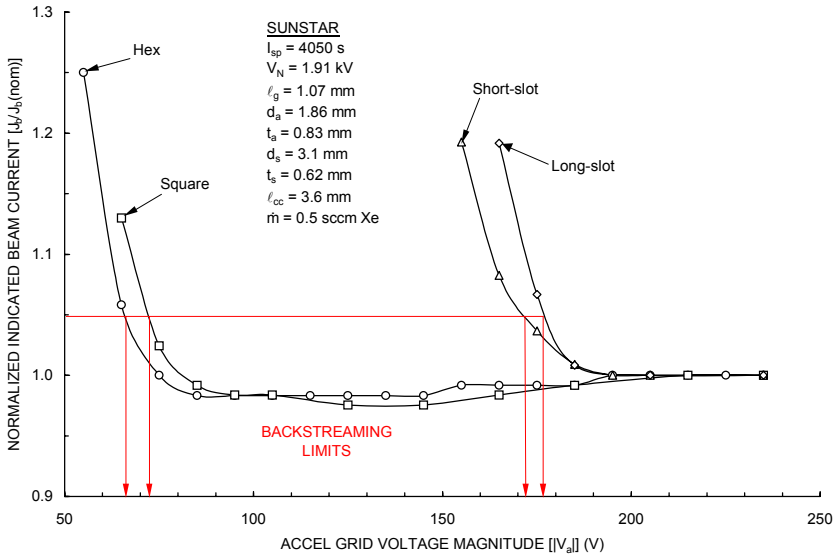

Fig. 4b Backstreaming limit data for the SUNSTAR gridlets throttled from 3000 to 6000 s.

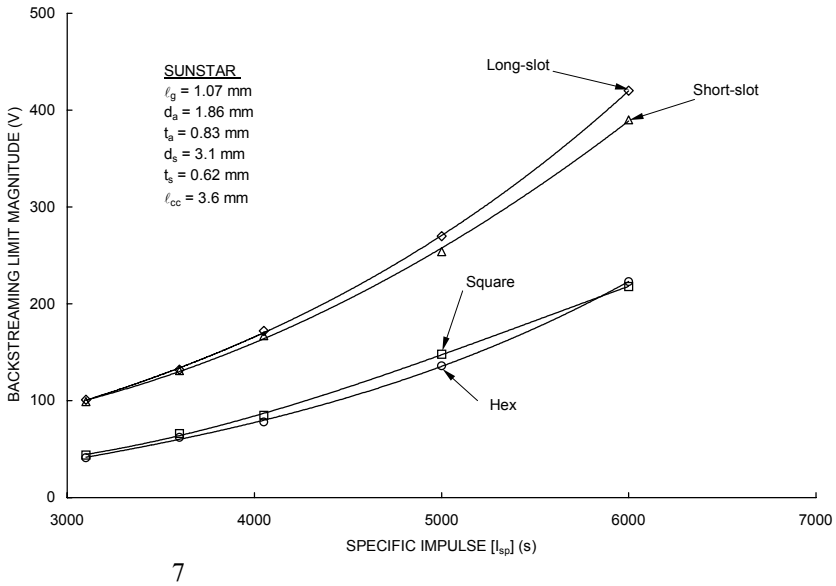

patterns are well below the value of 185 V predicted by the simple empirical backstreaming model of Ref. 4 for this geometry. Recall that poor agreement between model predictions and experimental measurements was also observed in experiments on the SHAG gridlets where significant effects of neutralizer operational conditions on backstreaming measurements were identified. A quick test was attempted using the SUNSTAR hex pattern grids to determine the effect of decreasing the neutralizer coupling bias from -15 V to -25 V on the ability to resist electron backstreaming. This ten volt decrease in coupling voltage was observed to cause the backstreaming limit to increase by ~34 V. Figure 4b contains backstreaming data plotted as a function of specific impulse. Again, the slotted apertures are observed to behavior similarly and they backstream at significantly higher voltage magnitudes than do the hex- and square-patterned, round-hole gridlets.

In addition to backstreaming limit evaluation, crossover and perveance limits were measured for the SUNSTAR gridlets in a manner similar to that used in Fig. 2a. Typical results are shown in Fig. 5a for the example case of the hex pattern gridlet operated over a specific impulse range from 3,100 s to 6,000 s. The data were analyzed by dividing the impingement current by the total beam current and plotting this ratio against beam current per unit of total screen grid area required for all holes ($J_B/A_{TG} = J_b/A_{tg}$). This same test was performed on the other three gridlets, and the data were used to determine crossover and perveance limits, which are plotted in Figs. 5b and 5c as functions of specific impulse. It is argued that the J_b/A_{tg} parameter yields values that are more representative of performance that would be observed in full-sized grid sets fabricated using the aperture geometry and hole or slot packing density of the individual SUNSTAR gridlets evaluated in this study. Although the slots outperformed the hex and square layout patterns in terms of total current density handling capability, the hex pattern displayed the greatest overall operating range between the crossover and perveance limits. This result suggests that the hex pattern would be well suited to missions requiring extensive throttling or for ion thrusters with poor beam flatness.

Considering the 4050-s specific impulse condition, it can be seen from Figs. 5b and 5c that the hex pattern results in an operating range of 0.5 to 3.1 mA/cm^2, the largest of the four SUNSTAR gridlets. Again, the crossover limits do not vary significantly between the hex and square patterns as they are both ~0.5 mA/cm^2, nor do they vary between the short- and long-slot patterns as they are both ~1.7 mA/cm^2. However, the perveance limits do vary between each of the configurations. At 4050 s, the long-slot pattern shows the highest perveance limit at 3.7 mA/cm^2, while the square pattern yields the lowest perveance limit at 2.9 A/cm^2. At higher specific impulses, the long slot pattern operating range is closer to that of the hex pattern, but recall that the backstreaming voltage is much worse. On the basis that higher accel voltage magnitudes will cause higher erosion rates, we argue that the long-slot pattern may not be as attractive for missions requiring ultra-long life. However, in this regard we note that innovative shaping of the accel hole geometry could improve the backstreaming performance of slotted grid geometries.[7]

Interstellar Precursor (IP) Ion Optics- High I_{sp}

Perveance and crossover limits were measured using 7-hole gridlets and computed using numerical simulation[1] for an ion optics system geometry being considered for high specific impulse, Interstellar-Precursor (IP) class ion thrusters. Results from tests for gridlets fabricated from both Poco graphite and carbon-carbon composite material operated at V_N = 13 kV are shown in Fig. 6a. For a net accelerating voltage of 13 kV, the numerical simulations predicted perveance limitations would occur at beamlet currents beyond about 5.4 mA (for a grid spacing of ℓg = 6.6 mm) and 7.5 mA (for a grid spacing of ℓg = 4.9 mm). Both experimentally measured perveance limits identified on Fig. 6a agree well with each other and the numerical simulation results. Note that the sudden upward wiggle in the base impingement level for the graphite gridlet set with the 6.6 mm spacing at ~5 mA was due to an increase in propellant flow rate that was required to reach the perveance limit.

Although the limits are in good agreement, the actual impingement-to-beamlet current ratios are vastly different between the experimental and numerical tests. This is because relatively high flow rates were needed to perform the tests and this resulted in high-test facility neutral densities and correspondingly high-charge-exchange-ion production rates. Even though the neutral background pressure was quite high, the experimental impingement currents measured between the crossover and perveance limits are mostly due to charge exchange ions that flow from a large region downstream of the accel grid rather than from regions within the beamlet. It is considered likely that the onset of significant direct impingement occurs during the experiments before the actual onset is detected due to the masking effect of the charge exchange flow from the downstream beam plasma. We believe that better experimental limit detection sensitivity may be possible if a third grid (placed downstream of the accel grid) was used to intercept most of the beam-plasma charge-exchange ion current.

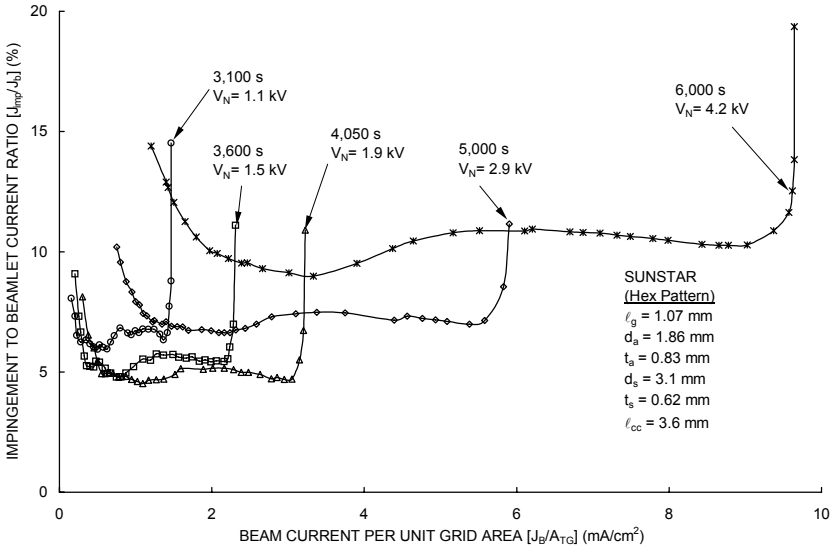

Fig. 5a Typical impingement current behavior for the hex pattern SUNSTAR gridlet versus specific impulse.

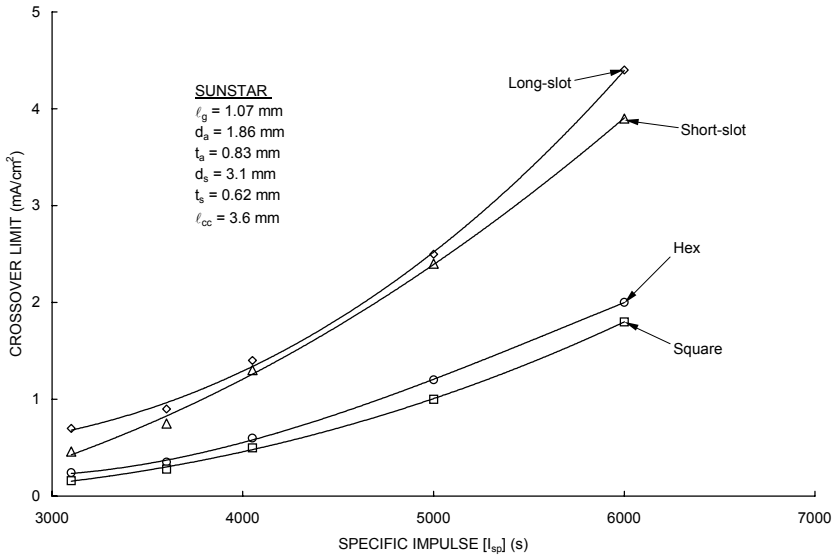

Fig. 5b Typical crossover limit behavior for the SUNSTAR gridlets versus specific impulse

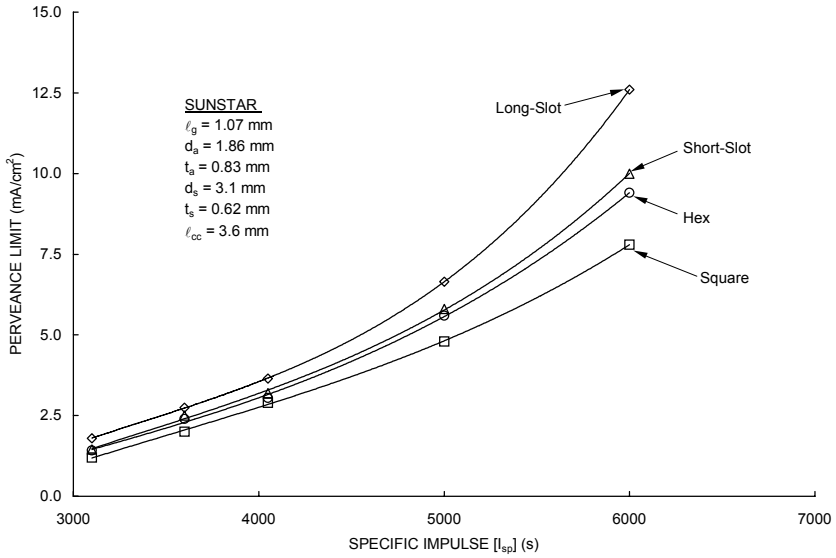

Fig. 5c Typical perveance limit behavior for the SUNSTAR gridlets versus specific impulse

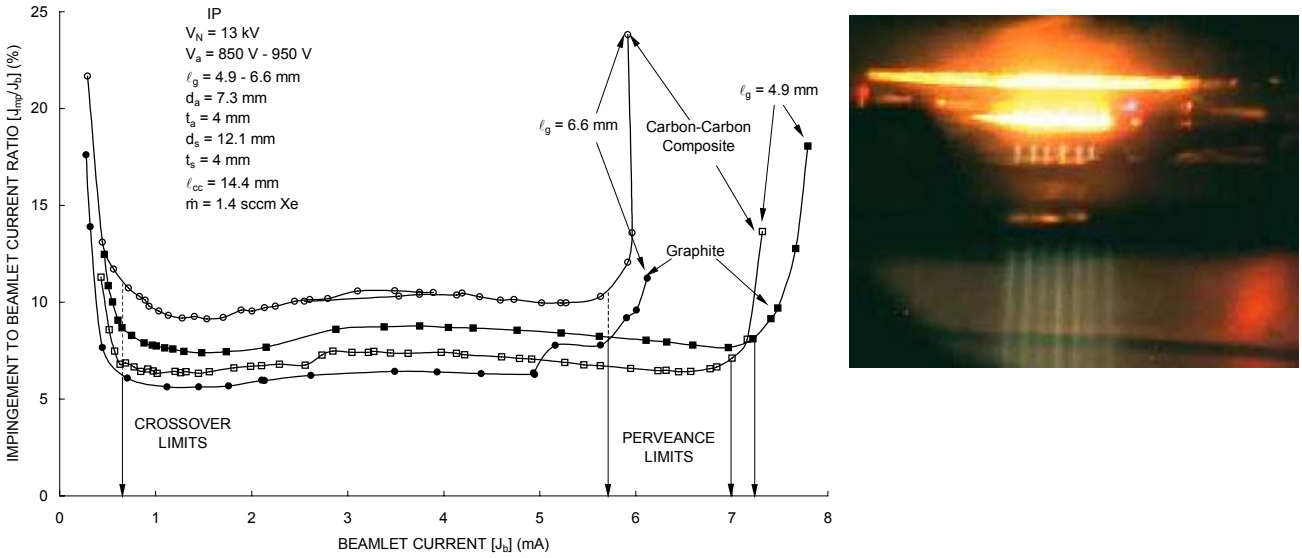

Fig. 6a Impingement current behavior for IP gridlets fabricated from graphite and carbon-carbon composite.

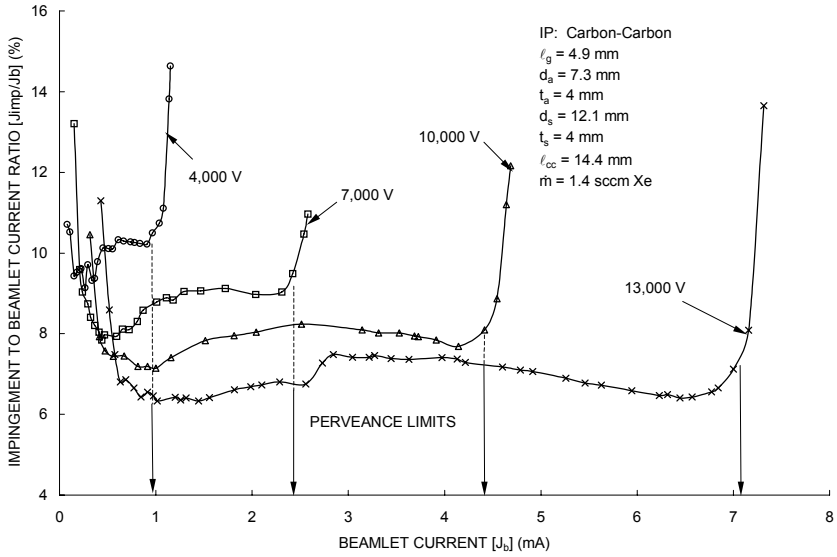

Fig. 6b Throttling affects on impingement current for IP gridlets.

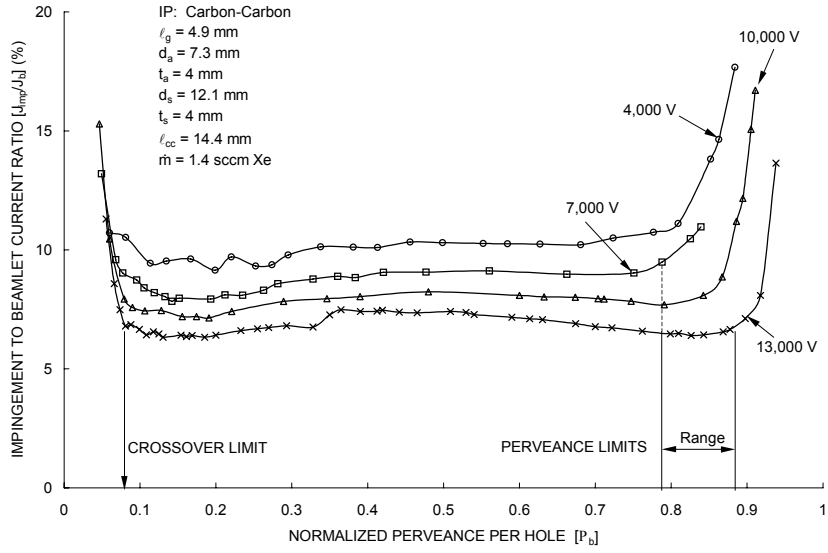

Fig. 6c Throttling affects on impingement current for IP gridlets normalized using perveance per hole.

Figure 6a also contains an inset photograph of the ion beamlets produced at 13 kV and J_b = 2 mA. The beamlets appeared to be hollow (i.e., light from the beamlet core appeared to be less intense than that from the annular region surrounding the core). It is possible that this observation was caused by an optical illusion, however, researchers at JPL have observed slightly hollow beamlet shapes in numerical simulations.[8]

Figure 6b shows relative impingement current results for the carbon-carbon IP gridlets at a 4.9 mm spacing over a wide range of net voltage conditions. As expected, the perveance limit increased significantly with the applied net voltage. The crossover current limit also increased slightly with applied voltage. Although both limits increase, the operating range between the impingement current limits increased as the applied voltage was increased. The same results were found for the IP gridlets at the larger spacing. Further analysis was done on the 4.9 mm spacing data in an attempt to normalize it to total voltage effects, and the data are re-plotted in Fig. 6c vs. normalized perveance per hole [Eq. (2)]. It can be seen that normalizing the data in this way results in reasonable congruity of the limits.

CONCLUSIONS AND RECOMMEDATIONS FOR FUTURE WORK

The range of non-direct ion impingement current collection to the accelerator grid of an ion thruster optics system is bounded by crossover and perveance limits, and sub-scale grids (gridlets) were used to determine these limits for a wide range of aperture geometries and sizes. In addition to limitations induced by operating conditions and geometrical design, strong perveance limitations were observed when hole-to-hole alignments were poor. Judged from the ease of conducting the tests, we feel that gridlet testing can provide a quick and cost effective method for performing both (1) proof-of-design demonstration and (2) baseline evaluation of numerical models. Computer controlled milling techniques were used to fabricate all of the gridlets evaluated in this study. The success of this technique suggests that future work could involve machining cusp features directly into the barrels of gridlet apertures to study metal grids fabricated using etching processes. In addition, simple and complex shaped slots can be evaluated quickly without going through the expensive of fabricating a full-sized grid set. This technique also allows the possibility of producing a series of gridlets with intentionally misaligned holes to simulate random and systematic hole misalignment that are experienced in the assembly of full-scale ion thruster optics systems. In separate testing, the neutralizer operating conditions were found to affect the onset of backstreaming substantially. In these tests, the use of a small plasma source to simulate a true plasma neutralizer was introduced. The neutralizer plasma probe could be operated over wide ranges of plasma production rate, flow rate, and bias condition, and was found to be a useful tool for performing backstreaming limit studies using SHAG gridlets. Future work will be to evaluate more fully SUNSTAR and IP grids under different neutralizer plasma probe conditions. Once this technique is fully developed, we plan to use it during tests of accel gridlets that have been machined with pits/grooves and enlarged apertures to simulate effects of grid erosion on performance.

ACKNOWLEDGMENT

Financial support from the Jet Propulsion Laboratory is gratefully acknowledged.

REFERENCES

[1] Y. Nakayama and P.J. Wilbur, "Numerical Simulation of High Specific Impulse Ion Thruster Optics," 27th International Electric Propulsion Conference, IEPC-01-099, Pasadena, CA, 2001.

[2] C.C. Farnell, J.D. Williams, and P.J. Wilbur, "Numerical Simulation of Ion Thruster Optics," International Electric Propulsion Conference, IEPC-03-073, Toulouse, France, 2003.

[3] J.E. Polk, J.R. Brophy, W. Shih, J. Beatty, D.M. Laufer, P.J Wilbur, and J.D. Williams, "Large Carbon-Carbon Grids for High Power, High Specific Impulse Ion Thrusters," Proceedings of the Space Technology and Applications International Forum, STAIF-2003, edited by M. el-Genk, AIP Conference Proceedings 654, New York, 2003.

[4] J.R. Beattie, J.D. Williams, and J.N. Matossian, "Ion Thruster with Long Lifetime Ion Optics System," U.S. Pat. No. 5,924,277, 1999.

[5] P.J. Wilbur, J. Miller, C.C. Farnell, and V.K. Rawlin, "A Study of High Specific Impulse Ion Thruster Optics," 27th International Electric Propulsion Conference, IEPC-01-098, Pasadena, CA, 2001.

[6] H.R. Kaufman, "Technology of Electron-Bombardment Ion Thrusters," appears in Advances in Electronics and Electron Physics, V. 36, Academic Press, San Francisco, pp. 300-302, 1974. See also K.R. Spangenberg, Vacuum Tubes, McGraw-Hill, New York, p. 348, 1948.

[7] J.S. Messole and M.E. Rorabaugh, "Fabrication and Testing of 15-cm Carbon-Carbon Grids with Slit Apertures," 30th Joint Propulsion Conference, AIAA-95-2661, 1995.

[8] J.R. Anderson, NASA Jet Propulsion Laboratory, private communication, Sept. 12, 2002.